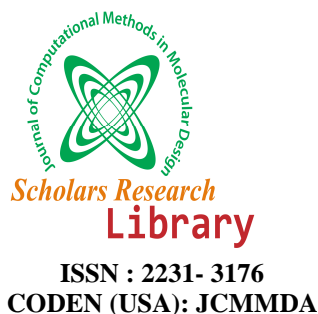




Scholars Research Library
(<http://scholarsresearchlibrary.com/archive.html>)



Quantum-chemical study of the relationships between electronic structure and anti- influenza activity. 2. The inhibition by 1H-1,2,3-triazole-4-carboxamide derivatives of the cytopathic effects produced by the influenza A/WSN/33 (H1N1) and A/HK/8/68 (H3N2) strains in MDCK cells

Diego Muñoz-Gacitúa and Juan S. Gómez-Jeria*

Quantum Pharmacology Unit, Department of Chemistry, Faculty of Sciences, University of Chile. Las Palmeras 3425, Santiago 7800003, Chile.

ABSTRACT

A formal quantum-chemical analysis of the relationships between molecular-electronic structure and the inhibition, by 1H-1,2,3-triazole-4-carboxamide derivatives, of cytopathic effects produced by the influenza A/WSN/33 (H1N1) and A/HK/8/68 (H3N2) strains in MDCK cells was carried out. The results suggest that the molecules bind to the nucleoprotein of both viral strains through the same mechanism. The mechanism has a very high orbital control as expected in highly complex recognition and binding processes. A short discussion about the existence of molecular orbitals is also presented.

INTRODUCTION

To date 18 HA subtypes (H1-H18) and 11 NA (N1-N11) subtypes of influenza A virus are known that infect both avian and mammalian species (see Ref. [1] for bibliography). These viruses have high mutation ability. One mechanism is through antigenic drift, the natural mutation over time of known strains of influenza. This can lead to a loss of antibody protection that may have developed after infection or vaccination with an older strain. Another mutation process is by antigenic shift. In this case two or more different strains of a virus, or strains of two or more different viruses, combine to form a new subtype having a combination of the surface antigens of the two or more original strains. Antigenic shift occurs only in influenza A virus because it infects more than just humans [2]. As affected species include birds and other mammals than man, this gives influenza A the opportunity for a major reorganization of surface antigens. Antigenic shift is a specific case of reassortment or viral shift that confers a phenotypic change. Reassortment is to blame for some of the most important genetic shifts in the history of the influenza virus [3, 4]. The 1957 and 1968 pandemic flu strains were produced by reassortment between an avian virus and a human virus. The H1N1 virus responsible for the 2009 swine flu outbreak has an unusual mix of swine, avian and human influenza genetic sequences [5]. The special receptiveness of pigs to infection with avian and mammalian influenza viruses, the close proximity of pigs and poultry farms, and the human practices of raising and trading of farm animals and farm animal products, offer opportunities for genetic exchange and interspecies transmission of influenza A viruses. Even though only H1 and H3 influenza subtypes have broadly circulated and caused disease in pig populations worldwide [6], the H9 subtype is being constantly detected in pigs in Asia, plus sporadic infections with highly pathogenic H5 avian influenza viruses. Swine viruses are continuously isolated from poultry species, especially turkeys. Today for most types of H_xN_y ($x=1, 18, y=1, 11$) viruses there is a plethora of strains infecting mammals and avian species [7-41].

One of the areas of research to combat influenza A is the design and testing of novel synthetic molecules with

enhanced antiviral activity. Today we have drugs inhibiting neuraminidase (zanamivir and oseltamivir) and M2 ion channel blockers (amantadine and rimantidine). A new target is the virus nucleoprotein (NP), encoded by the fifth genome segment expressed in abundance during the course of the infection [42-44]. NP is highly conserved. Recently a group of 1*H*-1,2,3-triazole-4-carboxamide derivatives was synthesized and tested for the inhibition of cytopathic effects (CPE) produced by influenza A/WSN/33 (H1N1) and A/HK/8/68 (H3N2) strains in MDCK cells. The target of these molecules seems to be the viral NP. In order to design new molecules with a broader spectrum of action we need experimental data comparing the antiviral activity against different viral strains [45]. Recently, we obtained promising results for a group of angelicin derivatives acting as inhibitors of the cytopathic effects produced by the influenza A/WSN/33 (H1N1) strain [46]. In part 1 of this series we presented formal quantitative structure-activity relationships for the inhibition of the cytopathic effects produced by the influenza A/Guangdong Luohu/219/2006 (H1N1) strain [1]. Here we present the results of a formal quantum-chemical analysis of the inhibition, by 1*H*-1,2,3-triazole-4-carboxamide derivatives, of the cytopathic effects (CPE) produced by the influenza A/WSN/33 (H1N1) and A/HK/8/68 (H3N2) strains in MDCK cells.

MATERIALS AND METHODS

The method.

The biological activity, $\log(A_i)$, is a linear function of several local atomic reactivity indices (LARIs) and has the following general form [47-52]:

$$\begin{aligned} \log A_i = & a + bM_{D_i} + c \log \left[\sigma_{D_i} / (ABC)^{1/2} \right] + \sum_j \left[e_j Q_j + f_j S_j^E + s_j S_j^N \right] + \\ & + \sum_j \sum_m \left[h_j(m) F_j(m) + x_j(m) S_j^E(m) \right] + \sum_j \sum_{m'} \left[r_j(m') F_j(m') + t_j(m') S_j^N(m') \right] + \\ & + \sum_j \left[g_j \mu_j + k_j \eta_j + o_j \omega_j + z_j \zeta_j + w_j Q_j^{\max} \right] \end{aligned} \quad (1)$$

where M is the drug molecule's mass, σ its symmetry number and ABC the product of the molecule's moment of inertia about the three principal axes of rotation. Q_j is the net charge of atom j , S_j^E and S_j^N are, respectively, the total atomic electrophilic and nucleophilic superdelocalizabilities of Fukui et al., $F_{j,m}$ ($F_{j,m'}$) is the Fukui index of the occupied (empty) MO m (m') localized on atom j . $S_j^E(m)$ is the atomic electrophilic superdelocalizability of MO m on atom j , etc. The total atomic electrophilic superdelocalizability of atom j corresponds to the sum over occupied MOs of the $S_j^E(m)$'s and the total atomic nucleophilic superdelocalizability of atom j is the sum over empty MOs of the $S_j^N(m)$'s. μ_j is the local atomic electronic chemical potential of atom j (the HOMO $_j^*$ -LUMO $_j^*$ midpoint), η_j is the local atomic hardness of atom j , ω_j is the local atomic electrophilicity of atom j , ζ_j is the local atomic softness of atom j (the inverse of η_j) and Q_j^{\max} is the maximal amount of electronic charge that atom j may accept from another site. HOMO $_j^*$ refers to the highest occupied molecular orbital localized on atom j and LUMO $_j^*$ to the lowest vacant MO localized on atom j . They are called the local atomic frontier MOs.

The moment of inertia term can be expressed as [49, 50]:

$$\log \left[(ABC)^{-1/2} \right] = \sum_t \sum_t m_{i,t} R_{i,t}^2 = \sum_t O_t \quad (2)$$

where the summation over t is over the various substituents of the molecule, $m_{i,t}$ is the mass of the i -th atom belonging to the t -th substituent, $R_{i,t}$ being its distance to the atom to which the substituent is bonded. The O_t 's are the Orientational Parameters of the substituent (see Part 1 of this series for more details).

We would like to add some words about the nature of this model. As far as we know, it is the only member of the class of model-based methods [53]. First, one should formulate one or more hypotheses about the nature of the process one intends to study. Next one must translate these hypotheses into mathematical statements (equations). Finally, one solves these mathematical statements, compares them with the available experimental information and analyzes the results to produce new knowledge. In our case we have started from the statistical-mechanical expression of the equilibrium constant. Next we have applied physically-based approximations to obtain a system of linear equations expressing the equilibrium constant as a function of a set of, generally speaking, reactivity indices. Nothing has been added to these equations. If the logic followed to build the model is right and the equilibrium constants have been correctly measured, then we expect the solution of the system of linear equations to provide a

correct understanding of the physical process. The model has been successfully applied to the study of a variety of *in vitro* drug-receptor systems [49, 54-69] and has shown predictive capabilities [56-58]. Note the fact that the solution of the linear equations provides an equation describing the variation of the set of values of the equilibrium constants in terms of the variation of the numerical values of the terms appearing in the equation. This indicates that we are obtaining only a partial knowledge of the whole drug-receptor interaction mechanism. As the system of linear equations cannot be solved because we do not have enough cases (i.e., equilibrium constants) we use statistics only as a tool to obtain the best possible equation. As S. R. Johnson has pointed out, “statistics must serve science as a tool; statistics cannot replace scientific rationality, experimental designs, and personal observation” [70]. Statistics must be a servant and not a queen. QSAR literature is plagued with papers where scientific understanding has been circumvented in favor of blind validation tests with low resulting information content [70]. Also there is a pandemic of papers using the general formula “biological activity = anything I can put here to use in a statistical analysis”. “Anything I can put here to use in a statistical analysis” refers to any molecular descriptor taken from the realms of classical chemistry, quantum chemistry or mathematics, or a mixture of them. In these cases the *knowledge* obtained about the phenomenon is close to zero. On the other hand, papers reporting the synthesis and experimental biological activity of a series of compounds are also bedeviled with loose statements about the relationships between structure and activity. “If we exchange substituent X for substituent Y, activity Z decreases” is their general form. Such statements are merely the verbal translation of experimental results usually presented in a Table and explain nothing. The situation becomes worse when these statements are accompanied by others of the kind “activity Z decreases because substituent Y has a stronger inductive effect than substituent X” (from Mid-20th Century Organic Chemistry). The lack of an understanding that, in general, biological activity is encoded in the entire molecular structure and that the mere substitution of a hydrogen atom by a methyl group can affect the whole electronic structure of the molecule (by adding several sigma molecular orbitals and also modifying the eigenvalue spectrum) and not only the area neighboring the point of substitution, leads to these simplistic analyses. For a clear understanding of molecular phenomena the use of quantum chemistry is mandatory. If we observe Eq. 1 we shall see that there is a large number of atomic reactivity indices. Future developments may well add one or two more indices but the actual set contains almost all the information about what an atom can do when facing a given environment. Now, we have suggested that Eq. 1 can also be employed to describe *any* biological activity. What is the rationale behind this statement? If a molecule must face more than one interaction in more than one site to exert its observed biological activity, the description of these interactions (within the framework of atom interactions) must be made in quantum chemical terms, and this is also done with the above reactivity indices. A theoretical representation of the passage through membranes by passive diffusion or similar complex phenomena was described a long time ago in terms of some reactivity indices appearing in Eq. 1. Satisfactory results have been obtained for a variety of molecular series and biological activities [1, 46, 71-75]. What if no satisfactory results are obtained? When considering *in vitro* equilibrium constants this happened to us on only one occasion [60]. There were able to show that the experimental values were not true equilibrium constants. In another case the common skeleton hypothesis was modified because in the set analyzed there were two subsets interacting in different ways [69]. TBIological activity is much more complex than *in vitro* behavior, however. If unsatisfactory SAR results are obtained one must consider at least a reformulation of the constitution of the common skeleton (see below) or the possibility that a subset of molecules exert their biological activity through different mechanisms. We found the latter to be true in a study of inhibitors of the bovine viral diarrhea virus (unpublished results). The last criticism is directed to those who still attempt to obtain meaningful QSARs from receptor binding affinities and /or biological activities of racemic mixtures. We have enough knowledge about the differences of receptor binding affinity and biological activities between optical isomers to state that results of this kind are often of little scientific use (obviously they serve to publish something, justify research project funds and/or get a Patent).

Selection of the experimental data.

The set analyzed is a group of 1*H*-1,2,3-triazole-4-carboxamide derivatives with inhibitory activities against replication of the influenza A/HK/8/68 (H3N2) and A/WS/33 (H1N1) strains. The anti-influenza activity was evaluated using MDCK cell-based cytopathic CPE assays. The selected molecules are shown in Figure 1 and Table 1.

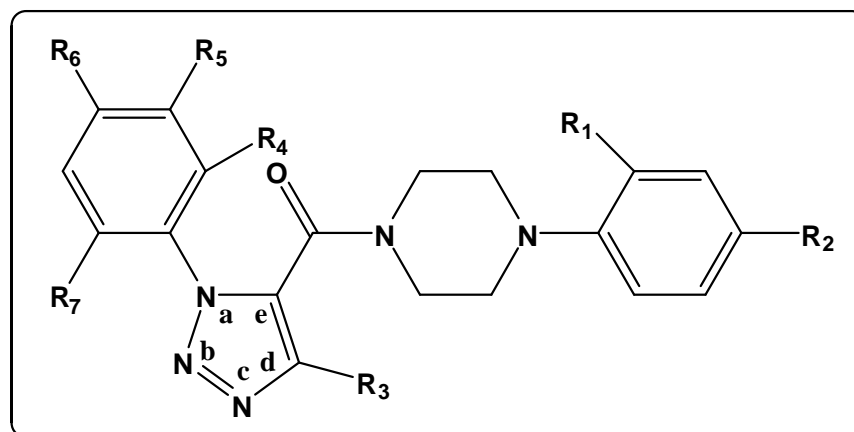


Figure 1. 1H-1,2,3-triazole-4-carboxamide derivatives.

Table 1. 1H-1,2,3-triazole-4-carboxamide derivatives and their anti-influenza activities.

Molecule		R ₁	R ₂	R ₃	R ₄	R ₅	R ₆	R ₇	log(IC ₅₀) H1N1	log(IC ₅₀) H3N2
js1*	1	Cl	NO ₂	CH ₃	H	H	H	H	-0.49	0.03
js2a*	2	Cl	NO ₂	CH ₃	H	H	H	H	0.68	0.78
js2b*	3	Cl	NO ₂	CH ₃	H	H	H	O C ₂ H ₅	-0.15	0.42
js4a*	4	Cl	NO ₂	CH ₃	H	H	H	H	0.53	0.94
js4b*	5	Cl	NO ₂	CH ₃	H	H	H	Cl	-0.14	0.46
js3a	6	Cl	NO ₂	CH ₃	H	H	H	H	0.50	0.71
js3b	7	Cl	NO ₂	CH ₃	OCH ₃	H	H	H	-0.17	0.29
js3c	8	Cl	NO ₂	CH ₃	H	O C ₂ H ₅	H	H	0.73	1.14
js3d	9	Cl	NO ₂	CH ₃	H	H	O C ₂ H ₅	H	0.75	1.17
js3e	10	Cl	NO ₂	CH ₃	Cl	H	H	H	0.08	0.75
js3f	11	Cl	NO ₂	CH ₃	H	Cl	H	H	0.69	0.97
js3g	12	Cl	NO ₂	CH ₃	H	H	Cl	H	0.69	--
js3h	13	Cl	NO ₂	CH ₃	OH	H	H	H	0.20	0.89
js3i	14	Cl	NO ₂	CH ₃	C ₂ H ₅	H	H	H	0.38	0.69
js3j	15	Cl	NO ₂	CH ₃	O C ₂ H ₅	H	H	H	0.51	0.95
js3k	16	Cl	NO ₂	CH ₃	OCH(CH ₃) ₂	H	H	H	0.93	1.21
js3l	17	Cl	NO ₂	CH ₃	COC ₂ H ₅	H	H	H	1.14	1.17
js3m	18	Cl	NO ₂	CH ₃	O C ₂ H ₅	H	H	O C ₂ H ₅	0.13	0.38
js3n	19	Cl	NO ₂	H	O C ₂ H ₅	H	H	H	0.92	--
js3p	20	Cl	H	C ₂ H ₅	O C ₂ H ₅	H	H	H	1.68	--
js3q	21	H	NO ₂	CH ₃	O C ₂ H ₅	H	H	H	1.23	--

In molecule 1 a=C, c=O, a-b and b-c are double bonds. In molecules 2a and 2b a=C, b=O, a-e and c-d are double bonds. In molecules 5a and 5b, a=c and a-b and d-e are double bonds.

Calculations.

The electronic structure of all the molecules was calculated within the Density Functional Theory (DFT) at the B3LYP/6-31g(d,p) level of the theory with full geometry optimization using the Gaussian suite [76]. Negative electron populations coming from Mulliken Population Analysis were corrected as usual [77]. Molecular orbitals and molecular electrostatic potentials (MEP) were depicted using GaussView and Molekel [78, 79]. Orientational parameters were calculated as usual [50]. Linear Multiple Regression Analysis (LMRA) techniques were used to find the best solution of the linear system of equations 1. A matrix was built containing the dependent variable (the inhibitory activity of each case), the orientational parameter of the substituents and the local atomic reactivity indices of all atoms of the common skeleton as independent variables. The Statistica software was used for LMRA [80]. We worked with the *common skeleton hypothesis* stating that there is a definite collection of atoms, common to all molecules analyzed, that accounts for nearly all the biological activity. The effect of the substituents consists in modifying the electronic structure of the common skeleton and influencing the right alignment of the drug through the orientational parameters. It is hypothesized that different parts or this common skeleton account for all the interactions leading to the expression of the inhibitory activity. The common skeleton for 1H-1,2,3-triazole-4-carboxamide derivatives is depicted in Fig. 2.

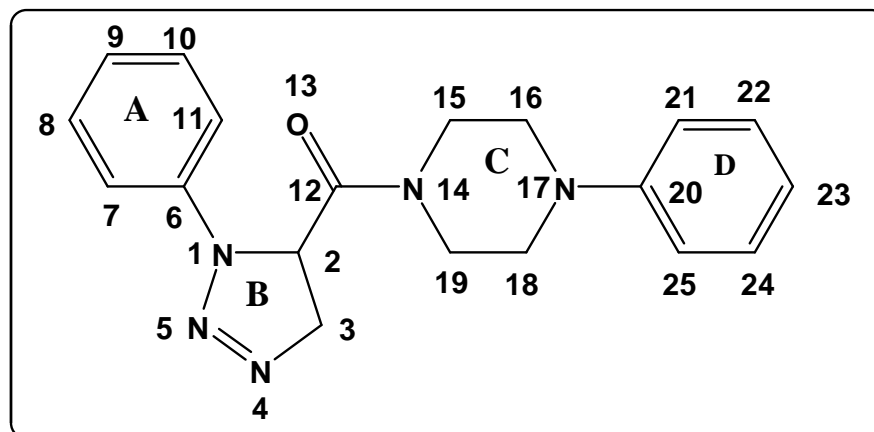


Figure 2. Numbering of atoms for the common skeleton of substituted 1H-1,2,3-triazole-4-carboxamide derivatives used in the LMRA.

RESULTS

Results for the inhibitory activity against influenza A/WS/33 (H1N1) strain replication.

The most statistically significant equation obtained is:

$$\log(IC_{50}) = 0.26 - 1.41F_5(LUMO + 2)^* - 0.04S_9^N(LUMO + 2)^* - 11.03F_{15}(HOMO - 1)^* + 3.84F_{15}(LUMO + 2)^* - 0.26S_{22}^E(HOMO - 1)^* + 0.005S_{25}^N(LUMO + 1)^* \quad (5)$$

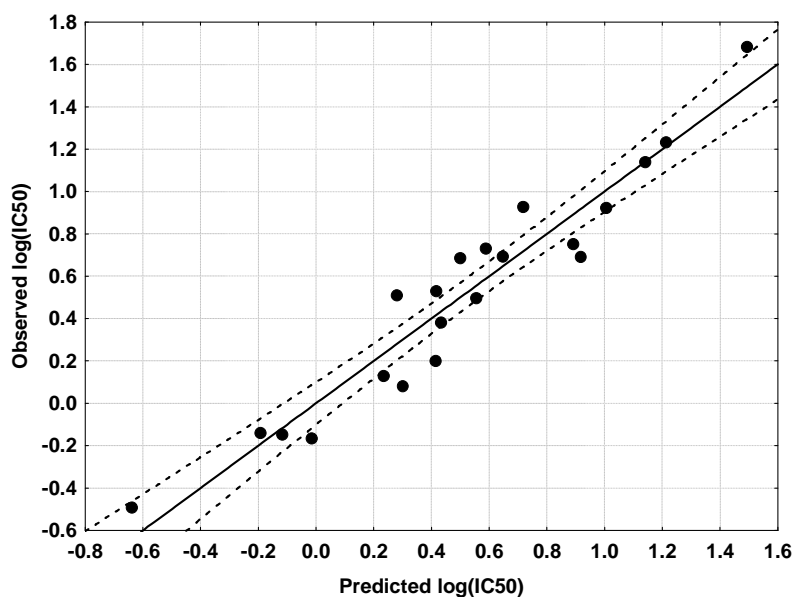
with $n=21$, $R=0.96$, $R^2=0.92$, $\text{adj } R^2=0.89$, $F(6,14)=54.17$ ($p<0.000001$), $\text{outliers}>2\sigma=0$ and $SD=0.18$. $S_9^N(LUMO + 2)^*$ is the local electrophilic superdelocalizability of the third highest local empty MO of atom 9. $S_{22}^E(HOMO - 1)^*$ and $S_{25}^N(LUMO + 1)^*$ have similar meanings, but for the first local highest occupied MO of atom 22 and the second local lowest empty MO of atom 25. $F_{15}(HOMO - 1)^*$ is the Fukui index of the second highest local MO of atom 15. $F_5(LUMO + 2)^*$ and $F_{15}(LUMO + 2)^*$ have similar meanings but for the third local empty MOs of atoms 5 and 15 respectively. The beta coefficients and t -test for the significance of coefficients of Eq. 5 are shown in Table 7. Concerning independent variables, Table 8 shows that there are no significant internal correlations. The associated statistical parameters of Eq. 5 show that this equation is statistically significant and that the variation of a group of local atomic reactivity indices belonging to the common skeleton explains about 89% of the variation of the inhibitory activity against influenza A/WS/33 (H1N1) strain replication. Figure 7 shows the plot of observed values vs. calculated ones.

Table 2. Beta coefficients and t -test for significance of coefficients in Eq. 5.

Variable	Beta	B	t(14)	p-level
$F_5(LUMO + 2)^*$	-0.36	-1.4125	-4.42	<0.0006
$S_9^N(LUMO + 2)^*$	-0.92	-0.0412	-11.44	<0.000001
$F_{15}(HOMO - 1)^*$	-0.24	-11.0337	-2.84	<0.013
$F_{15}(LUMO + 2)^*$	0.35	3.8442	4.26	<0.0008
$S_{22}^E(HOMO - 1)^*$	-0.27	-0.2592	-3.20	<0.006
$S_{25}^N(LUMO + 1)^*$	0.43	0.0045	4.91	<0.0002

Table 3. Squared correlation coefficients for the variables appearing in Eq. 5.

	$S_9^N(LUMO+2)^*$	$S_9^N(LUMO+2)^*$	$F_{15}(HOMO-1)^*$	$F_{15}(LUMO+2)^*$	$S_{22}^E(HOMO-1)^*$
$S_9^N(LUMO+2)^*$	0.006	1.00			
$F_{15}(HOMO-1)^*$	0.04	0.07	1.00		
$F_{15}(LUMO+2)^*$	0.002	0.003	0.003	1.00	
$S_{22}^E(HOMO-1)^*$	0.006	0.01	0.005	0.12	1.00
$S_{25}^N(LUMO+1)^*$	0.12	0.05	0.14	0.005	0.01

Figure 3. Plot of predicted vs. observed $\log(IC_{50})$ values from Eq. 5. Dashed lines denote the 95% confidence interval.

Results for the inhibitory activity against influenza A/HK/8/68 (H3N2) strain replication.

The most statistically significant equation obtained is:

$$\log(IC_{50}) = 0.79 - 0.95F_4(HOMO-2)^* + 0.004S_{21}^N - 0.0004\Theta_7 - 5.97F_{12}(HOMO-2)^* + 0.20S_8^E(HOMO-1)^* \quad (6)$$

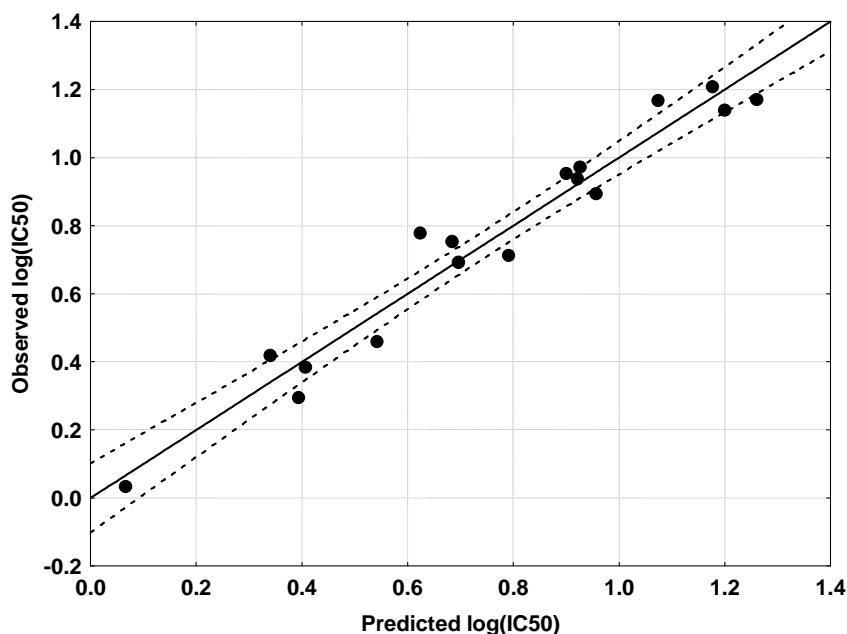
with $n=17$, $R=0.97$, $R^2=0.95$, $\text{adj } R^2=0.93$, $F(5,11)=44.41$ ($p<0.000001$), $\text{outliers}>2\sigma=0$ and $SD=0.09$. S_{21}^N is the total atomic nucleophilic superdelocalizability of atom 21. Θ_7 is the orientational parameter of the R_7 substituent. $S_8^E(HOMO-1)^*$ is the electrophilic superdelocalizability of the second highest local MO of atom 8. $F_4(HOMO-2)^*$ and $F_{12}(HOMO-2)^*$ are, respectively, the Fukui indices of the third highest occupied local MO of atoms 4 and 12 respectively. The beta coefficients and t -test for the significance of coefficients of Eq. 6 are shown in Table 9. Concerning independent variables, Table 10 shows that there are no significant internal correlations. The associated statistical parameters of Eq. 6 show that this equation is statistically significant and that the variation of a group of local atomic reactivity indices belonging to the common skeleton explains about 89% of the variation of the inhibitory activity against influenza A/HK/8/68 (H3N2) strain replication. Figure 8 shows the plot of observed values vs. calculated ones.

Table 4. Beta coefficients and t-test for significance of coefficients in Eq. 6.

Variable	Beta	B	t(11)	p-level
$F_4(HOMO-2)^*$	0.80	0.94942	10.77	<0.000001
S_{21}^N	0.70	0.00390	9.70	<0.000001
Θ_7	-0.59	-0.00368	-8.40	<0.000004
$F_{12}(HOMO-2)^*$	-0.37	-5.97024	-5.10	<0.0003
$S_8^E(HOMO-1)^*$	0.24	0.19981	3.28	<0.007

Table 5. Squared correlation coefficients for the variables appearing in Eq. 6.

	Θ_7	S_{21}^N	$F_{12}(HOMO-2)^*$	$S_8^E(HOMO-1)^*$
S_{21}^N	0.01	1.00		
$F_{12}(HOMO-2)^*$	0.07	0.05	1.00	
$S_8^E(HOMO-1)^*$	0.01	0.006	0.02	1.00
$F_4(HOMO-2)^*$	0.01	0.08	0.0009	0.14

Figure 4. Plot of predicted vs. observed $\log(IC_{50})$ values from Eq. 6. Dashed lines denote the 95% confidence interval.

DISCUSSION

Molecular electrostatic potential of the 1*H*-1,2,3-triazole-4-carboxamide derivatives.

Figure 5 shows that MEP of molecule 1 which is the one with the best antiviral activity against both influenza A strains. Figure 6 shows that MEP of molecule 20 which displays the lowest antiviral activity against H1N1 strain and no activity against H3N2 strain.

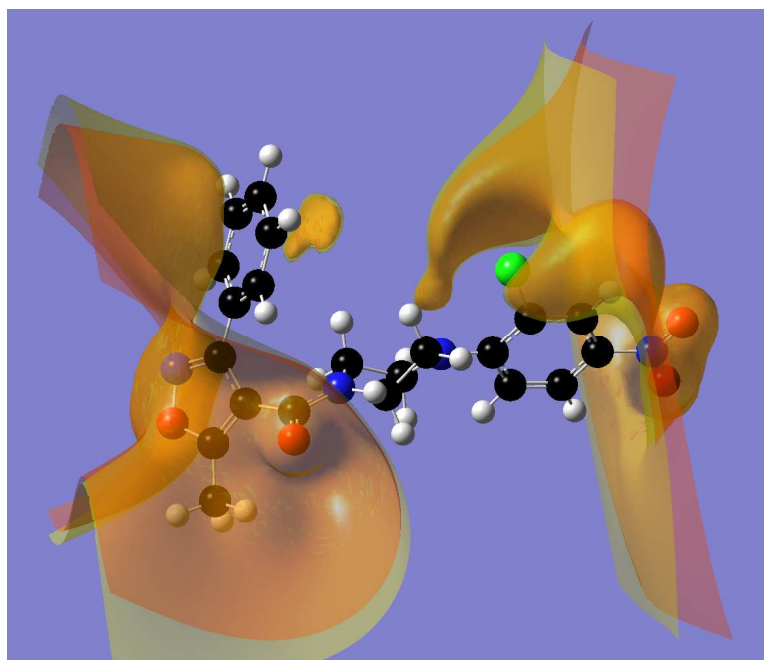


Figure 5. MEP of molecule 1. The orange isovalue surface corresponds to negative MEP values (-0.0004) and the yellow isovalue surface to positive MEP values (0.0004).

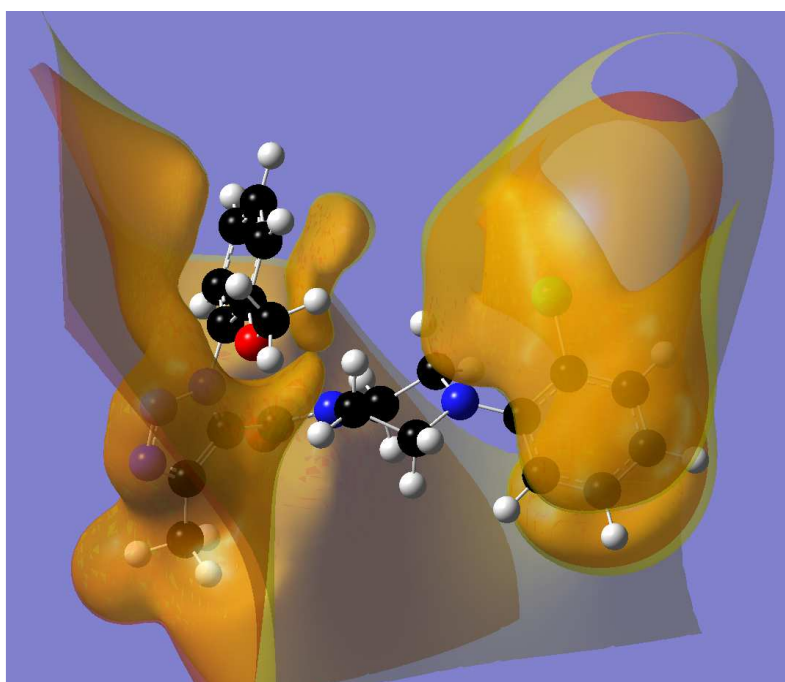


Figure 6. MEP of molecule 20. The orange isovalue surface corresponds to negative MEP values (-0.0004) and the yellow isovalue surface to positive MEP values (0.0004).

The structures of the MEP in the left side of Figs. 5 and 6 look similar. On the right hand side the MEP structure is more different, the negative MEP areas above and below the phenyl ring being very different. The question of what conformation these molecules may adopt for their long-range recognition by the partner cannot be answered for the moment. The simple superimposition of the molecular geometries of the set is not adequate. A good approach might be the study of the conformational space of all these molecules up to 7 kcal/mol to find a set of conformations with similar MEP structures, but the possibility of finding more than one set cannot be discarded. This requires a large computational effort that does not guarantee that, if we are in the presence of a multistep action mechanism, we will be able to correlate a particular MEP structure with a certain process. Figures 7 and 8 show, respectively, the MEP of molecules 1 and 18 at a distance of 4.5 Å from the nuclei.

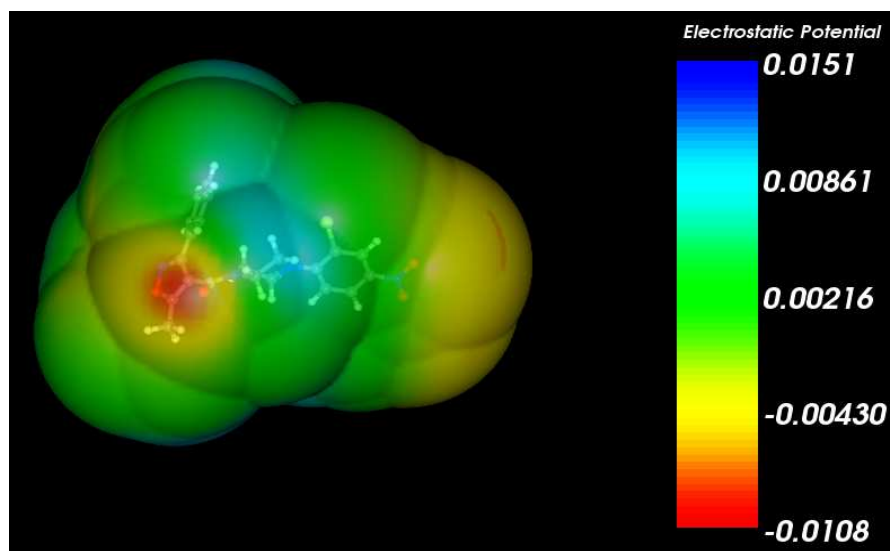


Figure 7. MEP of molecule 1 at 4.5 Å from the nuclei.

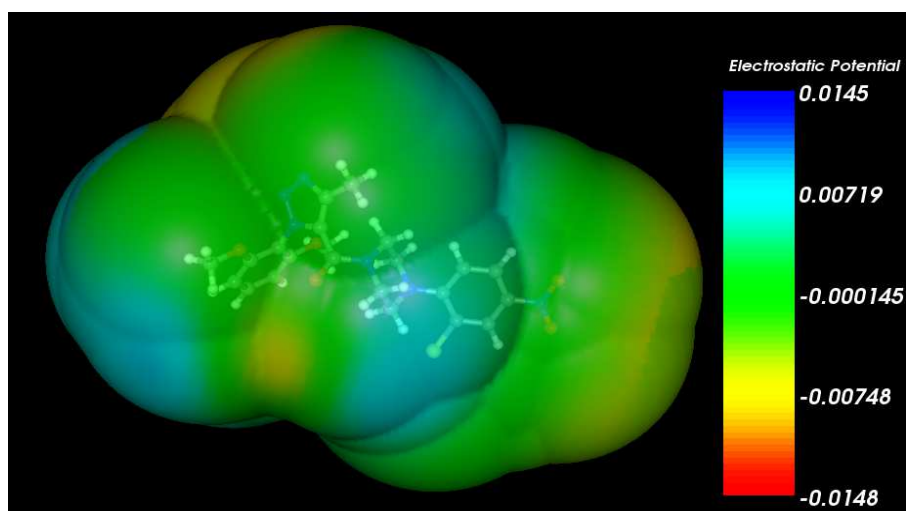


Figure 8. MEP of molecule 18 at 4.5 Å from the nuclei.

We may notice that the values of the MEP at this distance are smaller in molecule 8, but that the general structure of the MEPs is similar. At approximately this distance the recognition and orientation processes begin to occur.

Frontier molecular orbitals of the 1*H*-1,2,3-triazole-4-carboxamide derivatives.

Figures 9 and 10 show, respectively, the HOMOs of molecules 1 and 20.

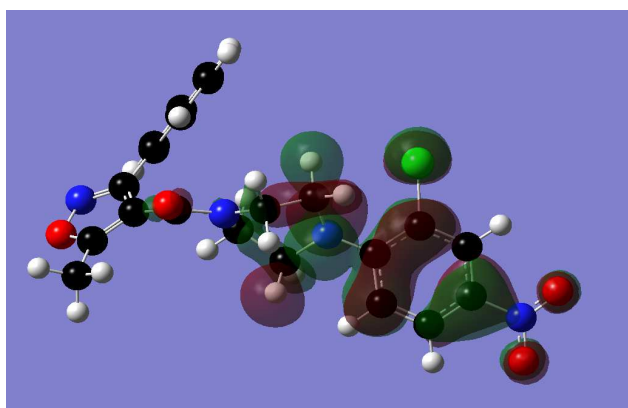


Figure 9. Localization of the highest occupied molecular orbital (HOMO) of molecule 1 (isovalue = 0.02).

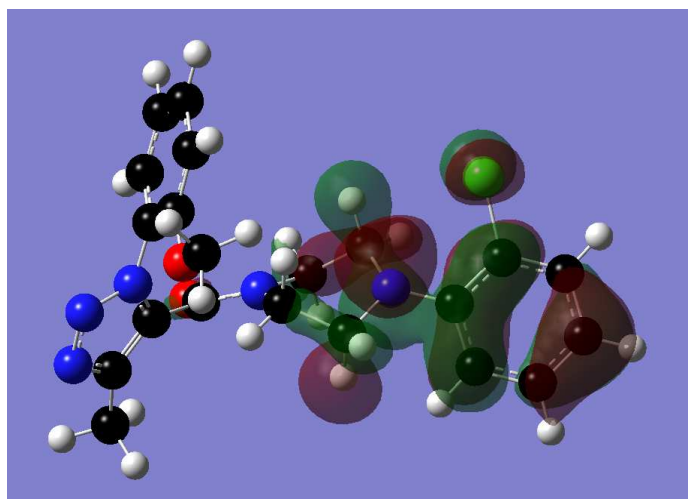


Figure 10. Localization of the highest occupied molecular orbital (HOMO) of molecule 20 (isovalue = 0.02).

In the case of molecule 1 the HOMO is localized on rings C (σ nature) and D (π nature), and on the chlorine atom. The same happens in the case of molecule 20. Then if these molecules are to donate charge they will do so from one or more atoms of ring D.

Figures 11 and 12 show, respectively, the LUMO of molecules 1 and 20.

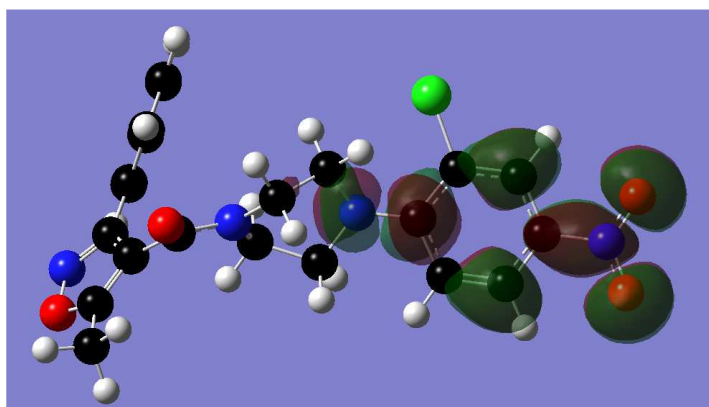


Figure 11. Localization of the lowest vacant (empty, unoccupied) molecular orbital (LUMO) of molecule 1 (isovalue = 0.02).

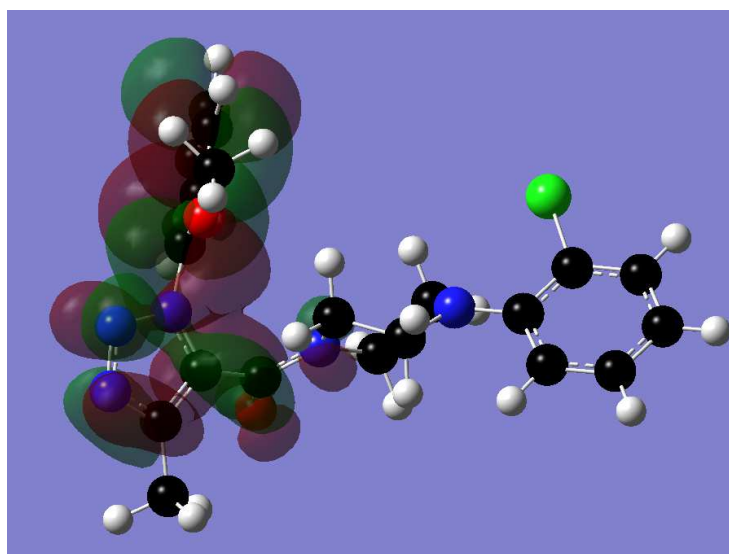


Figure 12. Localization of the lowest vacant molecular orbital (LUMO) of molecule 20 (isovalue = 0.02).

In molecule 1 the LUMO is localized mainly on ring D while in molecule 20 is localized on rings A and B. Both MOs are of π nature. This is a good example of how a single substitution can produce dramatic effects on the electronic structure of the whole system and justify part of the criticism made above. Then, if molecule 1 acts as an electron acceptor, electrons will be transferred to ring D. If ring D of molecule 20 should act also as an electron acceptor it will do so though the first vacant MO localized on it. On the hand, if a biological activity is linked to an electron transfer to ring A, molecule 20 can employ its LUMO while molecule 1 must employ the first vacant MO localized on it. Only the resolution of the system of linear equations 1 can give an insight into what might be happening.

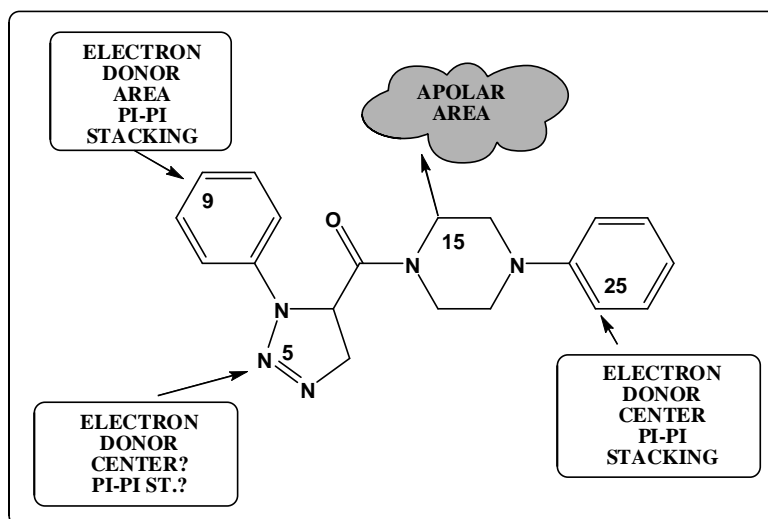


Figure 13. 2D pharmacophore for inhibition by 1H-1,2,3-triazole-4-carboxamide derivatives of the cytopathic effects produced by the influenza A/WSN/33 (H1N1) strain in MDCK cells.

Analysis of the relationship between molecular structure of the 1H-1,2,3-triazole-4-carboxamide derivatives and the inhibitory activity against influenza A/WS/33 (H1N1) strain replication (Eq. 5).

The variation of the inhibitory activity is related to the variation of six local atomic reactivity indices. The beta values (Table 2) indicate that the importance of these variables is $S_9^N(LUMO+2)^* > S_{25}^N(LUMO+1)^* > F_5(LUMO+2)^* = F_{15}(LUMO+2)^* > S_{22}^E(HOMO-1)^* = F_{15}(HOMO-1)^*$, these results being in agreement with the results of the *t*-test. Almost all points in Fig. 3 are within the 95% confidence interval suggesting that the common skeleton employed for the analysis is reliable. A basic variable-by-variable analysis of Eq. 5 suggests that a strong antiviral effect is mainly associated with high values for $F_5(LUMO+2)^*$ and with low values for $S_9^N(LUMO+2)^*$, $F_{15}(LUMO+2)^*$ and $S_{25}^N(LUMO+1)^*$. Considering the low beta values for $S_{22}^E(HOMO-1)^*$ and $F_{15}(HOMO-1)^*$, we shall abstain from doing a deeper analysis of these indices.

The whole process seems to be orbital-controlled [81-83]. As an example we shall employ molecule 1 in which the HOMO is the MO 111 and the LUMO the MO 112. The nature of the three highest occupied and three highest vacant local MOs is the following: atom 5 (108 π ,109 π ,110 π ,113 π ,115 π ,118 π), atom 9 (108 π ,109 π ,110 π ,113 π ,115 π ,116 π), atom 15 (108 σ ,109 σ ,111 σ ,121 σ ,124 σ ,125 σ) and atom 25 (101 π ,106 π ,111 π ,114 π ,117 π ,119 σ). The fact that MOs 108, 109 and 111 appear to be σ in some cases and π in others means that it has π nature on ring D and σ nature on ring C. Then, a high value for $F_5(LUMO+2)^*$ suggests that atom 5 may be directly interacting with an electron donor center or participating in a π - π stacking interaction with an aromatic moiety of the nucleoprotein. A low value for $S_9^N(LUMO+2)^*$ can be obtained by diminishing the localization of MO 116 on atom 9, by raising the associated eigenvalue or by both effects. This can be done by placing the appropriate substituent(s) in the correct place(s) (which are not necessarily atom 9 or ring A). With all these considerations and considering the fact that (LUMO+2) $_9^*$ and (LUMO+1) $_{25}^*$ are of π nature, we may tentatively speculate that a low localization of (LUMO+1) $_{25}^*$ and of (LUMO+2) on atom 9 may facilitate the interaction of their corresponding lower vacant MOs with electron-donor moieties or that they are participating in a π - π stacking interaction. In the case of atom 25, its local hardness (the HOMO $_{25}^*$ -LUMO $_{25}^*$ gap) is high (0.3 H, compare with 0.21 H, 0.21 H and 0.19 H for atoms 5, 9 and 15). The low value for $F_{15}(LUMO+2)^*$ could

indicate that atom 15 (and part or all of the piperazine moiety) is facing a non-polar area mainly composed by atoms having high local atomic hardnesses (i.e., a region with σ local frontier MOs, such as amino acid alkyl side chains for example). All these suggestions are depicted in the two-dimensional partial inhibition pharmacophore depicted in Fig. 13.

Analysis of the relationship between molecular structure of the 1*H*-1,2,3-triazole-4-carboxamide derivatives and inhibitory activity against influenza A/HK/8/68 (H3N2) strain replication (Eq. 6).

Here the variation of the inhibitory activity is related to the variation of five local atomic reactivity indices. The beta values (Table 4) indicate that the importance of these variables is $F_4(HOMO-2)^* > S_{21}^N > \Theta_7 > F_{12}(HOMO-2)^* > S_8^E(HOMO-1)^*$. Almost all points in Fig. 4 are within the 95% confidence interval suggesting that the common skeleton employed for the analysis is trustworthy. A variable-by-variable analysis of Eq. 4 indicates that a strong inhibitory activity is associated with high values for $F_4(HOMO-2)^*$, $F_{12}(HOMO-2)^*$, Θ_7 and $S_8^E(HOMO-1)^*$; and with low numerical values for S_{21}^N . A low numerical value for S_{21}^N indicates that atom 21 (on ring C) should have weak electron acceptor properties. This can be associated with a low or no localization of the molecular π MOs on atom 21, with increased eigenvalues of the low-lying vacant MOs, or with both. A high numerical value for the Θ_7 orientational parameter deserves some words. Orientational parameters depend exclusively on the mass and on the distance of the substituents' atoms to the centers to which they are attached. In a first and rudimentary approach, let us consider that the molecule can be considered as having fixed nuclei. At a given temperature we shall have a distribution of translational and rotational velocities. From classical mechanics we know that any three-dimensional rotation of a rigid body can be expressed in terms of rotations about its three principal axes. On the other hand, in a real situation we have continuous changes of the environment of the nucleoprotein and constant vibrations and/or rotations of some of its components. The arriving drug molecule needs a time interval, τ , to adapt to the environment in order to adopt an appropriate conformation to be recognized by its partner through long-range forces (the MEP is a useful tool to study this process). Only those molecules having the right mixture of translational and rotational velocities will achieve this process within τ . Now, if we relax the frozen nuclei condition and we accept that the set of molecules can adopt any conformation available from the fully optimized geometry up to 4-7 kcal/mol, the situation becomes really complex. Our first approach to use a substituent with a higher orientational parameter should be, for example, to replace a hydrogen atom by a methyl or ethyl substituent. But why not use a $C_{100}H_{201}$ substituent that is really big? This will not be useful because, in simple words, it will take more than τ to diminish the translational and rotational velocities of this molecule (think of the time needed to stop a 1.5 km long train traveling at 70 km/h). Then, there should be a range of substituents that can be used to achieve the goal of a higher orientational parameter. A second problem arises when substituting with larger and larger substituents. As an example, let us consider what happens when we change a methyl for an ethyl group. The orientational parameter will be higher but there will also be a change in the electronic structure of the whole system: eight electrons have been added which will contribute to the formation of core and σ molecular orbitals. A nitro substituent has a bigger orientational parameter value than the methyl group. The methyl group has nine electrons while the nitro group has 23 electrons. Besides, the nitro group has N-O π bonds. This substituent change will surely affect the π MO distribution and localization. Our practice has shown that some substitutions are able to change the localization of the π HOMO or π LUMO from an aromatic moiety to another, even if they do not belong to a common aromatic system (i.e. they are separated by saturated chains or rings). Then it seems that a working rule is to use substituents with similar electronic structures within a range of orientational parameter values (Tables with standard values are under preparation).

Atom 4 is located on ring B. A high value for $F_4(HOMO-2)^*$, a π MO, is indicative that this atom interacts as an electron donor (through an H-bond), or participates in a π - π stacking interaction. Given that atom 4 is an oxygen atom in some cases, the hypothesis of the hydrogen bond seems more plausible. A high value for $F_{12}(HOMO-2)^*$, a C atom forming a C=O bond, may be interpreted by saying that atom 12 is providing electrons to the bonded O atom and/or to B ring in the case that one of its atoms forms a hydrogen bond. Let us remember that, in a qualitative description, heavy atoms participating in an H-bond share (and therefore diminish) their electronic density and diminish their atomic net charge. This may provide the conditions to attract electrons from conjugated regions around them. Anyway the possibility of a bond of the C=O...H...X type is more plausible. A high value for $S_8^E(HOMO-1)^*$ suggests that atom 8 (on ring A) participates in a π - π stacking interaction with another aromatic moiety. Below we shall present a comment of what to do to transform these descriptions into more detailed statements. Figure 14 depicts the two-dimensional partial inhibition pharmacophore.

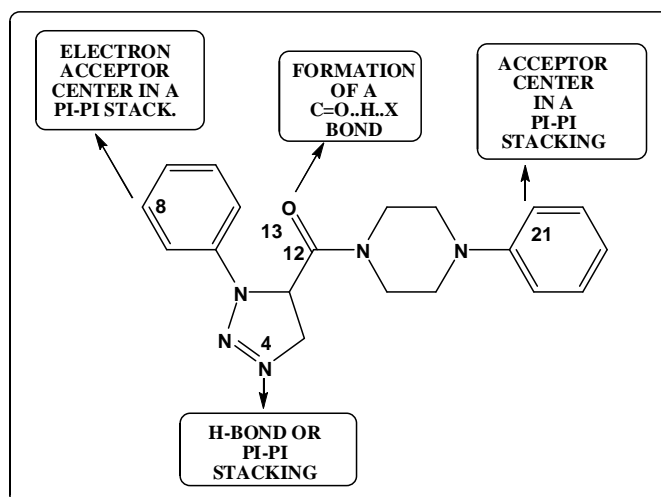


Figure 14. 2D pharmacophore for inhibition by 1H-1,2,3-triazole-4-carboxamide derivatives of the cytopathic effects produced by the influenza A/HK/8/68 (H3N2) strain in MDCK cells.

Now, if we compare Figures 13 and 14, we do not find any contradictions. Rings A and D seem to interact with the nucleoprotein through π - π stacking. Ring B could act through the same mechanism or by forming an H-bond. Oxygen 13 seems to form an H bond. Ring C interacts with a hydrophobic area. Recently, the X-ray crystal structure of compound 7 (shown in Fig. 15) bound to NP was solved with a resolution of 2.7 Å [84]. It was found that the structure contains two molecules of NP (NP-A and NP-B) and two molecules of compound in the asymmetric unit [84].

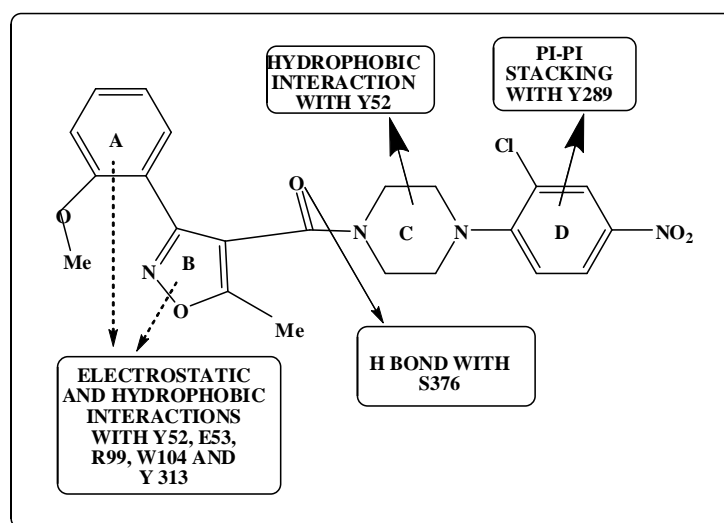


Figure 15. Compound 7 with some of the suggested interactions (from X-ray results).

From this X-ray structure, a frozen situation that is not necessarily the same as *in vitro*, the following suggestions were made:

1. Face-to-face π -stacking interactions are observed between the nitro-aryl moiety (Ring D) of compound 22 and Y289 of NP-A. This is fully consistent with our results.
2. The piperazine moiety of compound 22 (ring C) exhibits a hydrophobic interaction with Y52 of NP-B and an intramolecular hydrophobic interaction with the isoxazolyphenyl moiety of compound 22. The suggestion of a hydrophobic interaction is fully consistent with our results.
3. The amide carbonyl of compound 22 makes a strong H-bond with the side chain OH of S376 of NP-B and is conformationally stabilized by intramolecular electrostatic interactions with the oxygen of the methoxy group.
4. The isoxazole moiety (ring B) and its pendent aryl ring (ring A) fit into a well-defined pocket and engage in both electrostatic and hydrophobic interactions with residues Y52, E53, R99, W104, and Y313 of NP-B [84]. Maybe this is the correct interpretation for the frozen system, but our results indicate that ring A is engaged in a π - π stacking interaction and that ring B does the same or participates in H-bond formation.

As a general conclusion we may state that the results presented and discussed here are compatible with most of the experimental evidence regarding drug-NP interactions.

Now we shall discuss a rather complicated and sensitive matter. The existence and the form (if they exist) of the molecular orbitals is still a subject of controversy [85-88]. For example, in Woodward and Hofmann's paper on the conservation of orbital symmetry [89], examples are presented based on small molecules and the HOMO and LUMO (the latter is assumed to exist and to have the localization provided by a calculation). In these systems the location of the HOMO and the LUMO is easy to predict (think of the benzene molecule). We do not need to carry out calculations to know that occupied π MOs are localized on the carbon ring system and that σ MOs are localized between C-C and C-H bonded atoms. But in big molecules, such as the ones analyzed here, this is not a trivial endeavor. In practice we are working with vacant (or empty, or unoccupied) molecular orbitals assuming but never stating explicitly that they *exist*, that they *are there* and that *they have the nature and shape produced by a given calculation*. Curiously, all our work done on QSAR is compatible with these hidden facts. In their excellent paper Labarca and Lombardi analyze the relationship between quantum mechanics and quantum chemistry [85]. We cite. "As Amann claims, the innocent-looking Born–Oppenheimer approximation actually amounts to a 'declaration' that molecular chemistry smuggles into quantum mechanics: *'the nuclei of the involved molecule are declared to behave like classical particles'*". Therefore, the link between the chemical and the quantum description of the molecule is not a mere reductive relationship, to the extent that it involves a qualitative discontinuity between the related concepts [85]. We have commented on these issues because, despite the fact that the model used here has given excellent results in several systems, one of us (J.S.G.-J.) feels that something is still lacking to achieve a more detailed explanation of the drug-receptor interaction and complex biological activities.

REFERENCES

- [1] D Muñoz-Gacitúa; JS Gómez-Jeria, *J. Comput. Methods Drug Des.*, **2014**, in press.
- [2] J Ye; Y Xu; J Harris; H Sun; AS Bowman; F Cunningham; C Cardona; KJ Yoon; RD Slemons; X-F Wan, *Virol.*, **2013**, 446, 225-229.
- [3] X-S Zhang; D De Angelis; PJ White; A Charlett; RG Pebody; J McCauley, *Epidemics*, **2013**, 5, 20-33.
- [4] W Xu; Z Sun; Q Liu; J Xu; S Jiang; L Lu, *J. Infect.*, **2013**, 67, 490-494.
- [5] R Zu; L Dong; X Qi; D Wang; S Zou; T Bai; M Li; X Li; X Zhao; C Xu; X Huo; N Xiang; S Yang; Z Li; Z Xu; H Wang; Y Shu, *Virol.*, **2013**, 446, 49-55.
- [6] S Shikha Srivastava; N Misra; U Misra, *Der Pharm. Lett.*, **2009**, 1, 1-20.
- [7] X Xi; Q Fang; Q Gu; B Du, *J. Crit. Care*, **2013**, 28, 528-530.
- [8] V Wiwanitkit, *J. Chin. Med. Ass.*, **2013**, 76, 532.
- [9] AL Winter; A Eshaghi; DJ Farrell; A King; A Li; Y Li; JB Gubbay, *J. Clin. Virol.*, **2013**, 57, 279-281.
- [10] X-F Wan; M Carrel; L-P Long; AP Alker; M Emch, *Inf. Gen. Evol.*, **2013**, 20, 298-303.
- [11] A Vincent; L Awada; I Brown; H Chen; F Claes; G Dauphin; R Donis; M Culhane; K Hamilton; N Lewis; E Mumford; T Nguyen; S Parchariyanon; J Pasick; G Pavade; A Pereda; M Peiris; T Saito; S Swenson; K Van Reeth; R Webby; F Wong; J Ciacci-Zanella, *Zoon. Pub. Health*, **2013**, n/a-n/a.
- [12] D van Riel; LME Leijten; M de Graaf; JY Siegers; KR Short; MIJ Spronken; EJA Schrauwen; RAM Fouchier; ADME Osterhaus; T Kuiken, *Amer. J. Pathol.*, **2013**, 183, 1137-1143.
- [13] J van den Brand; K Stittelaar; G van Amerongen; L Reperant; L de Waal; A Osterhaus; T Kuiken, *J. Comp. Pathol.*, **2013**, 148, 56.
- [14] DH Tung; D Van Quyen; T Nguyen; HT Xuan; TN Nam; KD Duy, *Vet. Microbiol.*, **2013**, 165, 341-348.
- [15] I Tretyakova; MB Pearce; R Florese; TM Tumpsey; P Pushko, *Virol.*, **2013**, 442, 67-73.
- [16] Q Teng; X Zhang; D Xu; J Zhou; X Dai; Z Chen; Z Li, *Vet. Microbiol.*, **2013**, 162, 345-352.
- [17] R-B Tang; H-L Chen, *J. Chin. Med. Ass.*, **2013**, 76, 245-248.
- [18] Y Sun; S Sun; J Ma; Y Tan; L Du; Y Shen; Q Mu; J Pu; D Lin; J Liu, *Virol.*, **2013**, 435, 301-307.
- [19] X Sun; X Xu; Q Liu; D Liang; C Li; Q He; J Jiang; Y Cui; J Li; L Zheng; J Guo; Y Xiong; J Yan, *Inf. Gen. Evol.*, **2013**, 20, 471-475.
- [20] S Su; H-T Li; F-R Zhao; J-D Chen; J-x Xie; Z-M Chen; Z Huang; Y-M Hu; M-Z Zhang; L-K Tan; G-H Zhang; S-J Li, *Inf. Gen. Evol.*, **2013**, 14, 444-449.
- [21] M Stincarelli; R Arvia; MA De Marco; V Clausi; F Corcioli; C Cotti; M Delogu; I Donatelli; A Azzi; S Giannecchini, *Vir. Res.*, **2013**, 175, 151-154.
- [22] Q-q Song; F-x Zhang; J-j Liu; Z-s Ling; Y-l Zhu; S-j Jiang; Z-j Xie, *Vet. Microbiol.*, **2013**, 161, 331-333.
- [23] AP Ramos; BA Herrera; OV Ramírez; AA García; MM Jiménez; CS Valdés; AG Fernández; G González; SIO Fernández; GG Báez; BH Espinosa, *Int. J. Infect. Dis.*, **2013**, 17, e565-e567.
- [24] LJ Pérez; CL Perera; A Vega; MT Frías; D Rouseaux; L Ganges; JI Nuñez; H Díaz de Arce, *Res. Vet. Sci.*, **2013**, 94, 781-788.
- [25] BZ Löndt; SM Brookes; MD Kelly; BJ Nash; IH Brown, *Vet. Microbiol.*, **2013**, 162, 944-948.

- [26] S Liu; J Sun; J Cai; Z Miao; M Lu; S Qin; X Wang; H Lv; Z Yu; S Amer; C Chai, *J. Infect.*, **2013**, 67, 595-605.
- [27] Q Liu; L Lu; Z Sun; G-W Chen; Y Wen; S Jiang, *Microbes and Infection*, **2013**, 15, 432-439.
- [28] TT-Y Lam; J Wang; Y Shen; B Zhou; L Duan; C-L Cheung; C Ma; SJ Lycett; CY-H Leung; X Chen; L Li; W Hong; Y Chai; L Zhou; H Liang; Z Ou; Y Liu; A Farooqui; DJ Kelvin; LLM Poon; DK Smith; OG Pybus; GM Leung; Y Shu; RG Webster; RJ Webby; JSM Peiris; A Rambaut; H Zhu; Y Guan, *Nature*, **2013**, 502, 241-244.
- [29] CS Kyriakis; N Rose; E Foni; J Maldonado; WLA Loeffen; F Madec; G Simon; K Van Reeth, *Vet. Microbiol.*, **2013**, 162, 543-550.
- [30] JHCM Kreijtz; EJBV Kroeze; KJ Stittelaar; L de Waal; G van Amerongen; S van Trierum; P van Run; T Bestebroer; T. Kuiken; RAM Fouchier; GF Rimmelzwaan; ADME Osterhaus, *Vaccine*, **2013**, 31, 4995-4999.
- [31] J-i Kadota, *Respiratory Investigation*, **2013**, 51, 49.
- [32] JC Jones; T Baranovich; BM Marathe; AF Danner; JP Seiler; J Franks; EA Govorkova; S Krauss; RG Webster, *J. Virol.*, **2013**.
- [33] H-Y Jeoung; S-I Lim; B-H Shin; J-A Lim; J-Y Song; D-S Song; B-K Kang; H-J Moon; D-J An, *Vet. Microbiol.*, **2013**, 165, 281-286.
- [34] M Imai; S Herfst; EM Sorrell; EJA Schrauwen; M Linster; M De Graaf; RAM Fouchier; Y Kawaoka, *Vir. Res.*, **2013**, 178, 15-20.
- [35] Y Guan; GJD Smith, *Vir. Res.*, **2013**, 178, 35-43.
- [36] EA Govorkova; T Baranovich; P Seiler; J Armstrong; A Burnham; Y Guan; M Peiris; RJ Webby; RG Webster, *Antiv. Res.*, **2013**, 98, 297-304.
- [37] BB Dong; CL Xu; LB Dong; HJ Cheng; L Yang; SM Zou; M Chen; T Bai; Y Zhang; RB Gao; XD Li; JH Shi; H Yuan; J Yang; T Chen; Y Zhu; Y Xiong; S Yang; YL Shu, *Biomed. Envir. Sci.*, **2013**, 26, 546-551.
- [38] Y Chen; J Zhang; C Qiao; H Yang; Y Zhang; X Xin; H Chen, *Inf. Gen. Evol.*, **2013**, 13, 331-338.
- [39] G-W Chen; MMC Lai; S-C Wu; S-C Chang; L-M Huang; S-R Shih, *J. Formos. Med. Ass.*, **2013**, 112, 312-318.
- [40] A Badulak, *The Journal of Emergency Medicine*, **2013**, 45, 484.
- [41] G Zhao; Q Fan; L Zhong; Y Li; W Liu; X Liu; S Gao; D Peng; X Liu, *Res. Vet. Sci.*, **2012**, 93, 125-132.
- [42] W Zheng; YJ Tao, *FEBS Letters*, **2013**, 587, 1206-1214.
- [43] B Tarus; O Bakowicz; S Chenavas; L Duchemin; LF Estrozi; C Bourdieu; N Lejal; J Bernard; M Moudjou; C Chevalier; B Delmas; RWH Ruigrok; C Di Primo; A Slama-Schwok, *Biochimie*, **2012**, 94, 776-785.
- [44] EC Hutchinson; E Fodor, *Vaccine*, **2012**, 30, 7353-7358.
- [45] H Cheng; J Wan; M-I Lin; Y Liu; X Lu; J Liu; Y Xu; J Chen; Z Tu; Y-SE Cheng; K Ding, *J. Med. Chem.*, **2012**, 55, 2144-2153.
- [46] DA Alarcón; F Gatica-Díaz; JS Gómez-Jeria, *J. Chil. Chem. Soc.*, **2013**, 58, 1651-1659.
- [47] JS Gómez-Jeria, *Int. J. Quant. Chem.*, **1983**, 23, 1969-1972.
- [48] JS Gómez-Jeria, "Modeling the Drug-Receptor Interaction in Quantum Pharmacology," in *Molecules in Physics, Chemistry, and Biology*, J. Maruani Ed., vol. 4, pp. 215-231, Springer Netherlands, 1989.
- [49] JS Gómez-Jeria; M Ojeda-Vergara; C Donoso-Espinoza, *Mol. Engn.*, **1995**, 5, 391-401.
- [50] JS Gómez-Jeria; M Ojeda-Vergara, *J. Chil. Chem. Soc.*, **2003**, 48, 119-124.
- [51] JS Gómez-Jeria, *Elements of Molecular Electronic Pharmacology (in Spanish)*, Ediciones Sokar, Santiago de Chile, 2013.
- [52] JS Gómez-Jeria, *Canad. Chem. Trans.*, **2013**, 1, 25-55.
- [53] YC Martin, *Quantitative drug design: a critical introduction*, M. Dekker, New York, 1978.
- [54] JS Gómez-Jeria; D Morales-Lagos, "The mode of binding of phenylalkylamines to the Serotonergic Receptor," in *QSAR in design of Bioactive Drugs*, M. Kuchar Ed., pp. 145-173, Prous, J.R., Barcelona, Spain, 1984.
- [55] JS Gómez-Jeria; DR Morales-Lagos, *J. Pharm. Sci.*, **1984**, 73, 1725-1728.
- [56] JS Gómez-Jeria; D Morales-Lagos; JI Rodríguez-Gatica; JC Saavedra-Aguilar, *Int. J. Quant. Chem.*, **1985**, 28, 421-428.
- [57] JS Gómez-Jeria; D Morales-Lagos; BK Cassels; JC Saavedra-Aguilar, *Quant. Struct.-Relat.*, **1986**, 5, 153-157.
- [58] JS Gómez-Jeria; BK Cassels; JC Saavedra-Aguilar, *Eur. J. Med. Chem.*, **1987**, 22, 433-437.
- [59] JS Gómez-Jeria; P Sotomayor, *J. Mol. Struct. (Theochem)*, **1988**, 166, 493-498.
- [60] JS Gómez-Jeria; M Ojeda-Vergara, *Int. J. Quant. Chem.*, **1997**, 61, 997-1002.
- [61] JS Gómez-Jeria; L Lagos-Arancibia, *Int. J. Quant. Chem.*, **1999**, 71, 505-511.
- [62] JS Gómez-Jeria; L Lagos-Arancibia; E Sobarzo-Sánchez, *Bol. Soc. Chil. Quím.*, **2003**, 48, 61-66.
- [63] JS Gómez-Jeria; LA Gerli-Candia; SM Hurtado, *J. Chil. Chem. Soc.*, **2004**, 49, 307-312.
- [64] F Soto-Morales; JS Gómez-Jeria, *J. Chil. Chem. Soc.*, **2007**, 52, 1214-1219.
- [65] JS Gómez-Jeria; F Soto-Morales; J Rivas; A Sotomayor, *J. Chil. Chem. Soc.*, **2008**, 53, 1393-1399.
- [66] JS Gómez-Jeria, *J. Chil. Chem. Soc.*, **2010**, 55, 381-384.
- [67] T Bruna-Larenas; JS Gómez-Jeria, *Int. J. Med. Chem.*, **2012**, 2012 Article ID 682495, 1-16.
- [68] JS Gómez-Jeria, *Der Pharmacia Lettre*, **2014**, in press.,
- [69] F Salgado-Valdés; JS Gómez-Jeria, *J. Quant. Chem.*, **2014**, 2014 Article ID 431432, 1-15.
- [70] SR Johnson, *J. Chem. Info. Mod.*, **2007**, 48, 25-26.

- [71] C Barahona-Urbina; S Nuñez-Gonzalez; JS Gómez-Jeria, *J. Chil. Chem. Soc.*, **2012**, 57, 1497-1503.
- [72] JS Gómez-Jeria; M Flores-Catalán, *Canad. Chem. Trans.*, **2013**, 1, 215-237.
- [73] A Paz de la Vega; DA Alarcón; JS Gómez-Jeria, *J. Chil. Chem. Soc.*, **2013**, 58, 1842-1851.
- [74] I Reyes-Díaz; JS Gómez-Jeria, *J. Comput. Methods Drug Des.*, **2013**, 3, 11-21.
- [75] JS Gómez-Jeria, *Int. Res. J. Pure App. Chem.*, **2014**, 4, 270-291.
- [76] MJ Frisch; GW Trucks; HB Schlegel; et al., Gaussian98 Rev. A.11.3, Gaussian, Pittsburgh, PA, USA, 2002.
- [77] JS Gómez-Jeria, *J. Chil. Chem. Soc.*, **2009**, 54, 482-485.
- [78] RD Dennington; TA Keith; JM Millam, "GaussView 5.0.8," 340 Quinnipiac St., Bldg. 40, Wallingford, CT 06492, USA, 2000-2008.
- [79] U Varetto, Molekel 5.4.0.8, Swiss National Supercomputing Centre: Lugano, Switzerland, 2008.
- [80] Statsoft, Statistica 8.0, 2300 East 14 th St. Tulsa, OK 74104, USA, 1984-2007.
- [81] RF Hudson; G Klopman, *Tet. Lett.*, **1967**, 8, 1103-1108.
- [82] G Klopman; RF Hudson, *Theoret. Chim. Acta*, **1967**, 8, 165-174.
- [83] G Klopman, *J. Am. Chem. Soc.*, **1968**, 90, 223-234.
- [84] SW Gerritz; C Cianci; S Kim; BC Pearce; C Deminie; L Discotto; B McAuliffe; BF Minassian; S Shi; S Zhu; W Zhai; A Pendri; G Li; MA Poss; S Edavettal; PA McDonnell; HA Lewis; K Maskos; M Mörtl; R Kiefersauer; S Steinbacher; ET Baldwin; W Metzler; J Bryson; MD Healy; T Philip; M Zoeckler; R Schartman; M Sinz; VH Leyva-Grado; H-H Hoffmann; DR Langley; NA Meanwell; M Krystal, *Proc. Natl. Acad. Sci. USA*, **2011**, 108, 15366-15371.
- [85] M Labarca; O Lombardi, *Found. Chem.*, **2010**, 12, 149-157.
- [86] JF Ogilvie, *J. Chem. Ed.*, **1990**, 67, 280.
- [87] A Julg, *Int. J. Quant. Chem.*, **1984**, 26, 709-715.
- [88] A Julg, *Bull. Soc. Chim. Belg.*, **1976**, 85, 985-994.
- [89] R Hoffmann; RB Woodward, *Acc. Chem. Res.*, **1968**, 1, 17-22.